Plasma-photocatalytic conversion of CO_2 at low temperatures: Understanding the synergistic effect of plasma-catalysis

Danhua Mei[a], Xinbo Zhu[a], Chunfei Wu[b,c], Bryony Ashford[a], Paul T. Williams[b], Xin Tu[a, *]

[a] *Department of Electrical Engineering and Electronics, University of Liverpool, Liverpool, L69 3GJ, UK*

[b] *Energy & Resource Research Institute, University of Leeds, Leeds, LS2 9JT, UK*

[c] *School of Engineering, University of Hull, Hull, HU6 7RX, UK*

Corresponding Author

*Dr. Xin Tu

Department of Electrical Engineering and Electronics,

University of Liverpool,

Liverpool, L69 3GJ,

UK

Tel: +44-1517944513

E-mail: xin.tu@liverpool.ac.uk

Graphical abstract

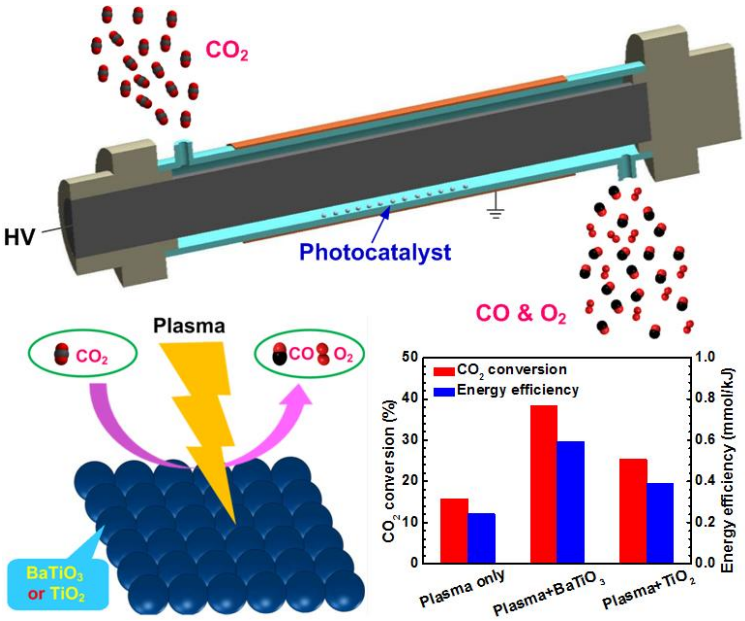

Abstract

A coaxial dielectric barrier discharge (DBD) reactor has been developed for plasma-catalytic conversion of pure CO_2 into CO and O_2 at low temperatures (<150 ^oC) and atmospheric pressure. The effect of specific energy density (SED) on the performance of the plasma process has been investigated. In the absence of a catalyst in the plasma, the maximum conversion of CO_2 reaches 21.7 % at a SED of 80 kJ/L. The combination of plasma with $BaTiO_3$ and TiO_2 photocatalysts in the CO_2 DBD slightly increases the gas temperature of the plasma by 6-11 ^oC compared to the CO_2 discharge in the absence of a catalyst at a SED of 28 kJ/L. The synergistic effect from the combination of plasma with photocatalysts ($BaTiO_3$ and TiO_2) at low temperatures contributes to a significant enhancement of both CO_2 conversion and energy efficiency by up to 250%. The UV intensity generated by the CO_2 discharge is significantly lower than that emitted from UV lamps that are used to activate photocatalysts in conventional photocatalytic reactions, which suggests that the UV emissions generated by the CO_2 DBD only play a very minor role in the activation of the $BaTiO_3$ and TiO_2 catalysts in the plasma-photocatalytic conversion of CO_2. The synergy of plasma-catalysis for CO_2 conversion can be mainly attributed to the physical effect induced by the presence of catalyst pellets in the discharge and the dominant photocatalytic surface reaction driven by the plasma.

Keywords: Plasma-catalysis; dielectric barrier discharge; CO_2 conversion; synergistic effect; energy efficiency

1. Introduction

Recently, the abatement of carbon dioxide (CO_2) has become a major global challenge as CO_2 is the main greenhouse gas and its emissions lead to the problems of climate change and global warming. Different strategies are being developed to tackle the challenges associated with CO_2 emissions, including carbon capture and storage (CCS), carbon capture and utilization (CCU), reducing fossil fuel consumption and boosting clean and renewable energy use. Direct conversion of CO_2 into value-added fuels and chemicals (e.g., CO, CH_4, and methanol) offers an attractive route for efficient utilization of low value CO_2 whilst significantly reducing CO_2 emissions [1]. However, CO_2 is a highly stable and non-combustible molecule, requiring considerable energy for upgrading and activation. Various synthetic approaches for CO_2 conversion have been explored, including solar driven photochemical reduction [2], electrochemical reduction [3] and thermal catalysis [4]. Despite their potential, further investigation into the development of cost-effective H_2 production methods, novel multifunctional catalysts and new catalytic processes are essential to improve the overall energy efficiency of CO_2 conversion processes and the product selectivity to practical and implementable levels.

Non-thermal plasma technology provides a promising alternative to the traditional catalytic route for the conversion of CO_2 into value-added fuels and chemicals at ambient conditions [5]. In non-thermal plasmas, highly energetic electrons and chemically reactive species (e.g., free radicals, excited atoms, ions, and molecules) can be generated for the initiation of both physical and chemical reactions. Non-thermal plasma has a distinct non-equilibrium character, which means the gas temperature in the plasma can be close to room temperature, whilst the electrons are highly energetic with a typical mean energy of 1-10 eV [6]. As a result, non-thermal plasma can easily

break most chemical bonds (e.g. C-O bonds), and enable thermodynamically unfavourable chemical reactions (e.g. CO_2 decomposition) to occur at ambient conditions. However, the use of plasma alone leads to low selectivity and yield towards the target end-products, and consequently causes low energy efficiency of the plasma processes. Recently, the combination of plasma with catalysis, known as plasma-catalysis, has attracted tremendous interest for environmental clean-up, greenhouse gas reforming, growth of carbon nanomaterials, ammonia synthesis and catalyst treatment [6-13]. The integration of plasma and solid catalysts has great potential to generate a synergistic effect, which can activate the catalysts at low temperatures and improve their activity and stability, resulting in the remarkable enhancement of reactant conversion, selectivity and yield of target products, as well as the energy efficiency of the plasma process [6]. Direct conversion of CO_2 into valuable CO and O_2 has been explored using different non-thermal plasmas [5, 14-25]. However, most previous works have mainly focused on the conversion of CO_2 diluted with noble gases (e.g. He and Ar), which is not preferable from an industrial application point of view [14, 22, 25]. Further fundamental work is still required to optimize and improve the energy efficiency of the plasma process. In addition, finding a suitable and cost-effective catalyst for this reaction to enhance the overall efficiency of the process is a great challenge as very limited work has been focused on plasma-catalytic CO_2 conversion. A detailed understanding of the synergistic effect resulting from the combination of plasma and photocatalysts at low temperature is still required due to gaps in current knowledge resulting in only a vague idea of the interactions occurring. For example, it is not clear what the roles are of UV light and highly energetic electrons generated by the plasma in the plasma-photocatalytic chemical reactions.

In this work, a coaxial dielectric barrier discharge (DBD) has been developed for the plasma-photocatalytic conversion of pure CO_2 into CO and O_2 at low temperature. The effect of photocatalysts ($BaTiO_3$ and TiO_2) on the temperatures (plasma gas temperature and the temperature on the catalyst surface) in the CO_2 DBD has been evaluated. The synergistic effect resulting from the combination of plasma and photocatalysts ($BaTiO_3$ and TiO_2) has been investigated from both physical and chemical perspectives.

2. Experimental

In this study, a coaxial dielectric barrier discharge (DBD) reactor has been developed for the plasma-catalytic reduction of pure CO_2 into CO and O_2 at atmospheric pressure and low temperatures (< 150 ^oC), as shown in Fig. 1. An Al foil (ground electrode) was wrapped around the outside of a quartz tube with an external diameter of 22 mm and an inner diameter of 19 mm. A stainless steel tube with an outer diameter of 14 mm was used as the inner electrode (high voltage electrode). The discharge gap was fixed at 2.5 mm, whilst the discharge length was varied from 90 to 150 mm. CO_2 was used as the feed gas without dilution at a flow rate of 15-60 mL/min. The DBD reactor was supplied by an AC high voltage power supply with a peak-to-peak voltage of 10 kV and a frequency of 50 Hz. All the electrical signals were sampled by a four-channel digital oscilloscope (TDS2014). Different catalyst pellets $BaTiO_3$ (TCU) and TiO_2 (*Alfa Aesar*) with a diameter of 1 mm were packed into the discharge gap along the bottom of the quartz tube. Our previous work demonstrated that this packing method induces effective plasma-catalyst interactions, which might generate a synergistic effect and hence promote plasma-catalytic chemical reactions [6]. The gas temperature and the temperature on the surface of the catalysts in the DBD reactor was measured by a fiber optical temperature probe

(Omega, FOB102), which was placed in the plasma area. X-ray diffraction (XRD) patterns of the fresh catalyst samples were recorded by a Siemens D5000 diffractometer using Cu-K_α radiation in the 2θ range between 10° and 70°. X-ray photoelectron spectroscopic (XPS) measurements were carried out on a Perkin-Elmer PHI-5400 XPS system with mono-chromatic Mg K_α (1253.6 eV) X-rays with a data acquisition system. The spectra are referenced to C1s peak at 284.5 eV. The UV intensity generated by the CO_2 DBD with and without a catalyst was measured by an UV meter (Omega HHUVA1). The gas products were analyzed by a two-channel gas chromatography (Shimadzu 2014) equipped with a flame ionization detector (FID) and a thermal conductivity detector (TCD). The concentration of ozone was measured by an ozone monitor (2B, Model 106-M). To evaluate the performance of the plasma process, the specific energy density (SED), CO_2 conversion (C_{CO2}), selectivity towards CO and O_2 (S_{CO} and S_{O2}), carbon and oxygen balance (B_{Carbon} and B_{Oxygen}) as well as energy efficiency (E) are defined as follows:

$$\mathrm{SED}\left(\mathrm{kJ/L}\right)=\frac{\text{Discharge power (kW)}}{\mathrm{CO_2\ flow\ rate\ (L/s)}} \tag{1}$$

$$C_{\mathrm{CO_2}}\left(\%\right)=\frac{\mathrm{CO_2\ converted\ (mol/s)}}{\mathrm{CO_2\ input\ (mol/s)}}\times 100 \tag{2}$$

$$S_{\mathrm{CO}}\left(\%\right)=\frac{\mathrm{CO\ produced\left(mol/s\right)}}{\mathrm{CO_2\ converted\left(mol/s\right)}}\times 100 \tag{3}$$

$$S_{\mathrm{O_2}}\left(\%\right)=\frac{\mathrm{O_2\ produced\left(mol/s\right)}}{\mathrm{CO_2\ converted\left(mol/s\right)}}\times 100 \tag{4}$$

$$B_{\mathrm{Carbon}}\left(\%\right)=\frac{\mathrm{CO_2\ unconverted\ (mol/s)+CO\ produced\left(mol/s\right)}}{\mathrm{CO_2\ input\left(mol/s\right)}}\times 100 \tag{5}$$

$$B_{\text{Oxygen}}(\%) = \frac{2\times CO_2 \text{ unconverted (mol/s)} + CO \text{ produced}\,(\text{mol/s}) + 2\times O_2 \text{ produced}\,(\text{mol/s})}{2\times CO_2 \text{ input}\,(\text{mol/s})} \times 100 \quad (6)$$

$$E\,(\text{mmol/kJ}) = \frac{CO_2 \text{ converted (mmol/s)}}{\text{Discharge power (kW)}} \quad (7)$$

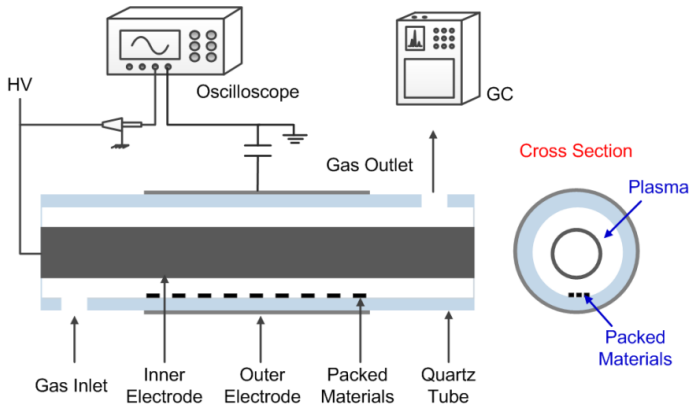

Fig. 1. Schematic diagram of the experimental setup

3. Results and Discussion

3.1. Plasma-assisted conversion of CO_2 without catalyst

Fig. 2 shows the effect of specific energy density (SED) on the conversion of CO_2 and the energy efficiency of the plasma reaction in the absence of a catalyst. Clearly, increasing the specific energy density significantly enhances CO_2 conversion due to the increase in energy input to the discharge. The conversion of CO_2 is increased by a factor of 3 (from 6.7% to 21.7%) as the SED rises from 8 kJ/L to 80 kJ/L. Similar conversion trends have been reported either using plasma alone or using plasma-catalysis for chemical reactions [26, 27]. Our previous works have shown that increasing energy input by changing applied voltage at a constant frequency could effectively increase the number of microdischarges and enhance the density of energetic electrons, as well as the gas temperature in the discharge [28-30], all of

which may contribute in different ways to the improvement in conversion. Moreover, increasing the discharge power produces more chemically reactive species (e.g. O atoms), which can further induce CO_2 dissociation to enhance its conversion. A lower feed gas flow rate was reported to be beneficial for improving the conversion of reactants due to longer retention time of the reactants in the plasma. In contrast, the specific energy density has an opposite effect on the energy efficiency of the plasma process. Increasing the SED from 8 kJ/L to 80 kJ/L leads to a decrease of the energy efficiency from 0.37 mmol/kJ to 0.12 mmol/kJ, which is consistent with previous results [31]. In this work, the maximum energy efficiency of 0.37 mmol/kJ is achieved at the lowest specific energy density of 8 kJ/L with a discharge power of 8 W, a CO_2 feed flow rate of 60 mL/min and a discharge length of 150 mm.

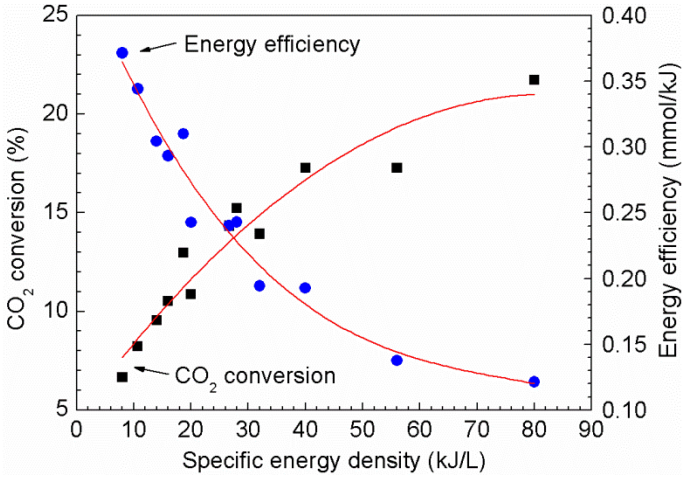

Fig. 2. CO_2 conversion and energy efficiency as a function of SED

CO_2 dissociation by electron impact vibrational excitation (Eqs 8-9) is believed to be the most effective pathway for CO_2 conversion in non-thermal plasmas, which can lead to a high energy efficiency of more than 60% [32].

$$e + CO_2 \rightarrow e + CO_2 (v^*) \quad (8)$$

$$e + CO_2 (v^*) \rightarrow e + CO + O \quad (9)$$

Where v^* is the vibrational excited state. Up to 97% of the total plasma energy can be transferred from electrons to vibrational excitation of CO_2 if the plasma discharges have an electron temperature of 1-2 eV, or a reduced electric field (E/N) of 20–40 Td [32]. Recent plasma modeling of CO_2 splitting in a DBD reactor showed that in a CO_2 discharge with an average electron energy of 2-3 eV, only 12% of the energy can be allocated to vibrational states, whereas ~79% goes to electronic excited states, and ~4% and ~5% can be transferred to dissociation and ionization of CO_2, respectively [33]. Their results showed that the majority (94%) of CO_2 conversion is induced by reactions (e.g. dissociation) with ground state CO_2 (shown in Eq. 10) and only 6% of CO_2 conversion occurs through reactions with vibrational excited CO_2 at a high electric field [33].

$$e + CO_2 \rightarrow e + CO + O \quad (10)$$

In this study, the average electric field E in the CO_2 DBD without a catalyst is estimated to be around 1.75 kV/mm under our experimental conditions, obtained from Lissajous figure [10], while the corresponding mean electron energy of the plasma is around 2.4 eV, calculated using BOLSIG+ code based on electron energy distribution function (EEDF) [34]. This result suggests that the electron impact dissociation of CO_2 might play a dominant role in CO_2 conversion in this experiment.

The electron impact dissociation of CO_2 in its vibrational excited states (Eq. 9) or ground state (Eq. 10) will most likely result in CO in its ground state ($^1\Sigma$) and O atoms in both the ground state (^3P) and metastable state (^1D). However, since CO bands were observed in the emission spectra of the CO_2 discharge generated in a similar coaxial DBD reactor, CO could also be formed in excited states [6].

Oxygen can be formed from the three-body recombination of atomic oxygen (Eq. 11) or from the reaction with a ground state CO_2 molecule (Eq. 12).

$$O + O + M \rightarrow O_2 + M \quad (11)$$

$$O + CO_2 \rightarrow CO + O_2 \quad (12)$$

Oxygen might also be generated directly by electron impact dissociation of CO_2 if the electron has a high energy (> 15 eV).

$$e + CO_2 \rightarrow C + O_2 + e \quad (13)$$

In this study, no carbon deposition is observed after the plasma conversion of CO_2 with and without catalyst. The main gas products from plasma conversion of pure CO_2 were CO and O_2. The selectivities towards CO and O_2 are in the range of 91.5%-96.7% and 45.4%-48.5%, respectively, while the carbon balance (98.1%-99.5%) and oxygen balance (98.0%-99.6%) are very high. This agrees with recent experimental and modelling works in which CO and O_2 were identified as the main products in the conversion of CO_2 when using DBD [33, 35]. Ozone could be formed by the following reaction:

$$O + O_2 + M \rightarrow O_3 + M \quad (14)$$

However, ozone was not detected in this work. Ozone could be decomposed by local heating generated by the plasma in the reactor. Andrev and co-workers suggested that oxygen formed from CO_2 dissociation could be initially converted into O_3, followed by ozone decomposition into O_2 through electron impact reactions [36]. In contrast, recent plasma modelling of CO_2 conversion showed that the calculated fractional density of O_3 was only 0.05% in a similar DBD reactor [33]. In addition, the maximum rate for ozone formation in the DBD reactor was two orders of magnitude lower than that of the three-body recombination of atomic oxygen for O_2 production

[33]. It is worth noting that gas heating was not calculated explicitly in the model, which might be able to explain the difference in ozone formation in the experiment and modelling. Our previous study has shown the formation of CO and CO_2^+ spectra in a similar DBD containing CO_2 using optical emission spectroscopic diagnostics [6], which suggests electron impact ionization of CO_2 occurs in the plasma CO_2 reaction.

$$e + CO_2 \rightarrow e + e + CO_2^+ \quad (15)$$

The recorded CO_2^+ spectra also reveal the formation of highly energetic electrons in the CO_2 discharge as the electron impact ionization of CO_2 requires electrons with a high energy of at least 13.8 eV.

3.2. Plasma-photocatalytic conversion of CO_2

The effect of $BaTiO_3$ and TiO_2 photocatalysts on the conversion of CO_2 is shown in Fig. 3. It is clear that the presence of both $BaTiO_3$ and TiO_2 in the discharge significantly enhances the CO_2 conversion and energy efficiency of the plasma process. Packing $BaTiO_3$ pellets into the discharge gap exhibits exceptional performance with a remarkable enhancement of both CO_2 conversion (from 15.2% to 38.3%) and energy efficiency (from 0.24 mmol/kJ to 0.60 mmol/kJ) by a factor of 2.5 at a SED of 28 kJ/L.

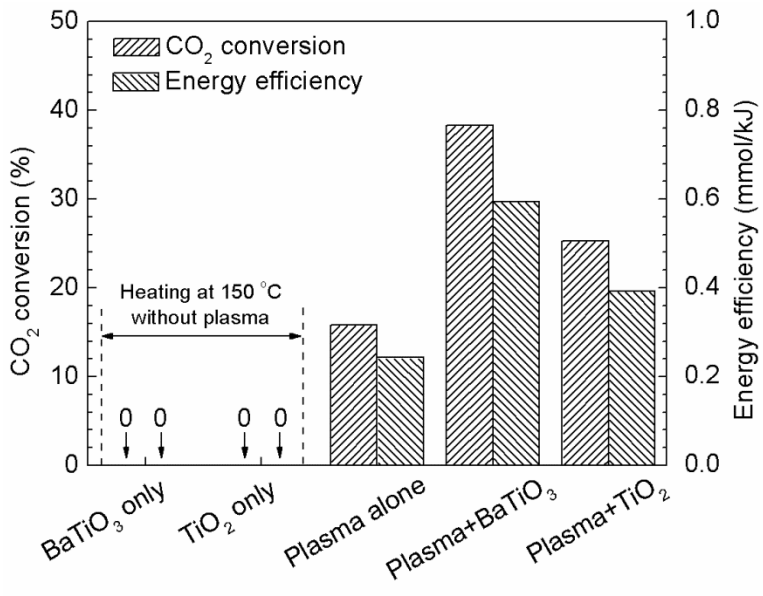

Fig. 3. Demonstration of the synergistic effect of plasma-catalysis for the conversion of CO_2 (SED = 28 kJ/L)

The plasma gas temperature and the temperature on the catalyst surface in the plasma conversion of CO_2 have been measured in the DBD reactor at a SED of 28 kJ/L, as shown in Fig. 4. Clearly, the plasma gas temperature of the CO_2 DBD without a catalyst significantly increases from 23.3 ^oC to 123.5 ^oC in the first 15 min after igniting the plasma, after which it rises slowly and is almost constant (~138 ^oC) at 25 min when the plasma reaches a stable state. Similar evolution behaviour of the temperature can also be observed in the plasma-catalysis system (Fig. 4). In the CO_2 DBD reactor partially packed with the $BaTiO_3$ and TiO_2 catalysts, we note that the plasma temperature in the gas phase and the temperature on the catalyst surface are almost the same. Thus, only one temperature (the temperature on the catalyst surface) is shown in Fig.4 to present the temperature in the plasma-catalysis system. It is interesting to note that the combination of plasma with the $BaTiO_3$ and TiO_2 catalysts slightly increases the gas temperature (TiO_2: ~144 ^oC and $BaTiO_3$: ~149 ^oC) of the CO_2 discharge by 6-11 ^oC compared to the CO_2 DBD in the absence of a catalyst at

the same SED of 28 kJ/L. This phenomenon might be attributed to inelastic electron-molecule collisions in the plasma-catalytic processes [12, 37, 38].

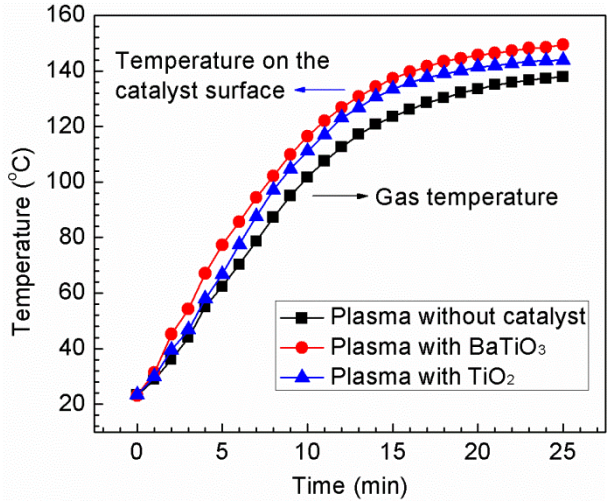

Fig. 4. Plasma gas temperature and the temperature on the surface of $BaTiO_3$ and TiO_2 catalysts in the CO_2 DBD reactor (SED = 28 kJ/L). Note that the gas temperature of the CO_2 DBD and the temperature on the catalyst surface are almost the same when the catalyst ($BaTiO_3$ and TiO_2) is placed in the plasma zone.

To understand the role of plasma in the reaction, a purely thermal experiment has been carried out by heating both photocatalysts in a pure CO_2 flow at 150 ^oC. No conversion and adsorption of CO_2 was observed. Thermodynamic equilibrium calculation of the CO_2 reaction has also confirmed that the conversion of CO_2 is almost zero at low temperatures (e.g., 150 ^oC), suggesting that an extremely low CO_2 conversion is expected from the thermal catalytic reduction of CO_2 when carried out at the same temperature as that used in the plasma reaction (see Fig. SI1 in the Supporting Information). The results clearly show that the exceptional reaction performance has been achieved by the use of plasma-catalysis, which is much higher

than the sum of plasma-alone and catalysis alone, indicating the formation of a synergistic effect when combining plasma with photocatalysts at low temperatures.

Catalysts can be integrated into a DBD system in different ways. The presence of the catalyst pellets in part of the gas gap still shows predominantly filamentary discharges and surface discharges on the catalyst surface, which induces effective interactions between plasma and catalyst for CO_2 activation. In this work, the dielectric constant of $BaTiO_3$ and TiO_2 is 10000 and 85, respectively. Previous experimental [39, 40] and simulation [41, 42] studies have shown that packing catalyst pellets, especially pellets with a high dielectric constant (e.g., $BaTiO_3$), into the discharge gap can generate a non-uniform electric field with enhanced electric field strength near contact points between the pellets and the pellet-dielectric wall. The maximum local electric field near these contact points can be much higher than that in the void in a plasma-catalysis reactor, depending on the contact angle, curvature and dielectric constant of the materials [43]. The space (including the space filled with pellets) averaged electric field in a plasma fully packed with packing pellets is initially increased by a factor of 1.4 when increasing the dielectric constant of the materials from 10 to 1000, above this the change in the electric field becomes negligible [43]. We have reported that the interaction of plasma and TiO_2 exhibited a strong effect on the electron energy distribution in the discharge with an increase in both highly energetic electrons and electric field [29]. This phenomenon can also be confirmed by previous work, showing that the presence of TiO_2 in a plasma leads to a significant increase of the reduced electric field [44]. These results suggest that the presence of the catalyst pellets in the plasma gap play a crucial role in inducing physical effects, such as enhancement of the electric field and production of more energetic electrons and reactive species, which in turn leads to chemical effects and contributes to the conversion of CO_2. In this study,

283 the average electric field is increased by 9.0% and 10.9% with the presence of $BaTiO_3$
284 and TiO_2 in the discharge gap, respectively; whilst the corresponding mean electron
285 energy is increased by 9.4% and 11.3% (see Fig. SI2 in the Supporting Information).
286 Both of these effects contribute to the enhancement of the CO_2 conversion.

287 However, the enhancement of the reaction performance in terms of CO_2 conversion
288 and energy efficiency is found to be more significant than only due to the changes in
289 plasma physical parameters (e.g. average electric field). This suggests that in addition
290 to the plasma physical effect and the resulting gas phase reactions (Eqs. 8-15), the
291 contribution of a plasma-activated photocatalytic reaction to the synergy of plasma-
292 catalysis cannot be ruled out. The XRD patterns of the samples show that $BaTiO_3$ has
293 the tetragonal phase, while TiO_2 exhibits the crystal structure of anatase (see Fig. SI3
294 in the Supporting Information). TiO_2 is a widely used photocatalyst with a wide band
295 gap of 3.2 eV for anatase phase, while $BaTiO_3$ is a perovskite semiconductor
296 photocatalyst with a band gap of 2.8-3.0 eV for tetragonal phase. It is well known that
297 photocatalysts can be activated through the formation of electron-hole (e^--h^+) pairs
298 with the aid of sufficient photonic energy ($h\nu$) with an appropriate wavelength to
299 overcome the band-gap between the valence band and the conductive band [45]:

300 $$TiO_2 + h\nu \rightarrow e^- + h^+ \quad (16)$$

301 $$BaTiO_3 + h\nu \rightarrow e^- + h^+ \quad (17)$$

302 Plasma discharges can generate UV radiation without using any extra UV sources (e.g. UV
303 lamps). This has been confirmed by the dominated N_2 (C-B) bands (between 300 nm and 400
304 nm) in a CO_2 DBD in our previous work [6, 46]. However, UV radiation generated by plasma
305 discharges is not always the controlling factor to activate photocatalysts due to its low
306 intensity compared to that emitted by an UV lamp [47]. In this work, we have measured the
307 UV intensity generated by the CO_2 DBD with and without a catalyst, as shown in Fig. 5. In

the absence of a catalyst in the DBD reactor, the UV intensity produced by the CO_2 discharge is about 0.141 mW/cm^2 at a SED of 28 kJ/L. When the $BaTiO_3$ and TiO_2 photocatalysts are placed in the plasma zone, the UV intensity of the CO_2 discharge is decreased to 0.115 mW/cm^2 and 0.123 mW/cm^2, respectively. Note that these values are significantly lower than the UV intensity (~20-60 mW/cm^2) produced from UV lamps to activate photocatalysts in conventional photocatalytic reactions [48-50], which suggests that the UV emissions generated by the CO_2 discharge only play a minor role in the activation of the $BaTiO_3$ and TiO_2 photocatalysts. Similar results have been reported in the previous papers [51, 52]. Assadi et al found that the UV light generated by a surface DBD was too weak to activate TiO_2 photocatalyst for the removal of 3-methylbutanal (3MBA) [51]. Sano et al reported that the UV intensity emitted by a N_2/O_2 surface discharge was only 2.5 μW/cm^2 at an input power of 5 W. The contribution of the plasma UV activated photocatalytic reaction to the overall performance of acetaldehyde decomposition was less than 0.2% [52].

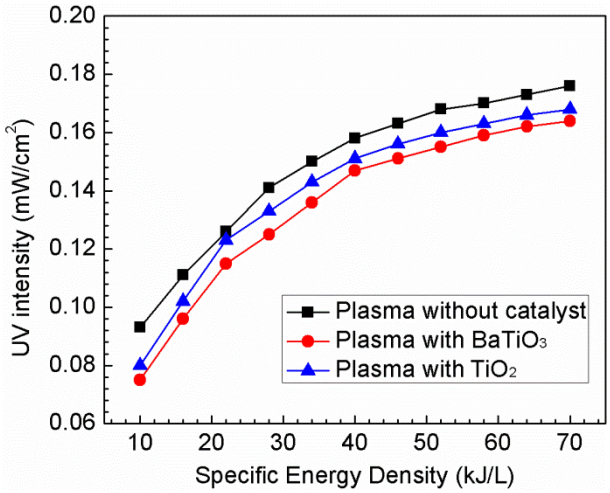

Fig. 5. UV intensity generated by the CO_2 DBD with and without a catalyst as a function of SED

Whitehead has suggested that electron-hole pairs can be created by electron impact upon the surface of photocatalysts since DBD can generate electrons of very similar energy (3 - 4 eV) to the photons [13, 53], as shown in Eqs. 18-19. Nakamura et al have also reported that photocatalysts can be activated by plasma and the electrons can be trapped onto the formed oxygen vacancies (V_o) to enhance the photoexcitation process [54].

In this work, the exceptional performance of the plasma-catalytic CO_2 conversion has been achieved through the combination of plasma and photocatalysts. However, the significant enhancement of the reaction performance in terms of CO_2 conversion and energy efficiency cannot only be attributed to the changes in plasma physical parameters (e.g. increased average electric field), as the estimated average electric field and mean electron energy in the CO_2 DBD are only increased by around 10% when the $BaTiO_3$ and TiO_2 catalysts are placed in the plasma zone. Furthermore, we find that the UV radiation generated by the CO_2 DBD is significantly weak compared to that produced from UV lamps, which suggests that it might only play a minor role in the activation of photocatalytic CO_2, and its contribution to the exceptional performance of the plasma-catalytic reaction and the synergy of plasma-photocatalysis could be very weak or negligible. In this study, the highly energetic electrons generated by plasma are considered as the main driving force to activate the photocatalysts for CO_2 conversion.

$$TiO_2 + e^- (>3.2\ eV) \rightarrow e^- + h^+ \quad (18)$$

$$BaTiO_3 + e^- (>3.0\ eV) \rightarrow e^- + h^+ \quad (19)$$

Previous investigation has shown that the photocatalytic conversion of CO_2 is a multistep process, which involves the adsorption and subsequent activation of CO_2 molecules on the surface of photocatalysts and the subsequent dissociation of the C-O

bond. The key step is the activation of CO_2 molecules through the transfer of trapped electrons to adsorbed CO_2 molecules in the V_o [55].

However, the recombination rate of electron-hole pairs is 2 or 3 orders of magnitude faster than that of charge separation and transfer in a defect-free photocatalyst, which will limit the efficiency of CO_2 conversion [55]. The defect disorders in photocatalysts, such as V_o, play an important role in the CO_2 reduction processes. V_o has been considered as the active site for the adsorption and activation of reactants in a photocatalytic reaction [56]. In this study, XPS measurement has been performed to investigate the surface structure and element valence of the photocatalysts. Fig. 6(a) shows the deconvolution spectra of Ti 2p in the $BaTiO_3$ sample. Two components (Ti $2p_{3/2}$ and Ti $2p_{1/2}$) are identified and can be deconvoluted into 4 peaks. Two peaks at higher binding energy (459.88 and 465.57 eV) are assigned to the formal valence of Ti (4+) in $BaTiO_3$; whilst the Ti $2p_{3/2}$ and Ti $2p_{1/2}$ peaks of Ti^{3+} are located at around 457.85 eV and 463.67 eV. The presence of Ti^{3+} in the $BaTiO_3$ sample demonstrates the formation of V_o on the catalyst surface through the following reaction [57, 58]:

$$2Ti^{4+} + O^{2-} \rightarrow V_o + 2Ti^{3+} + 1/2\ O_2 \quad (20)$$

where O^{2-} is the lattice oxygen. Clearly, the formation of V_o is followed by the change in the oxidative state of the vicinal Ti from Ti^{4+} to Ti^{3+} to retain the balance of local charge. Similarly, the Ti $2p_{3/2}$ and Ti $2p_{1/2}$ peaks of Ti^{3+} can also be detected in the XPS profile of TiO_2, as shown in Fig. 6(b). We find that there are more Ti^{3}+ species in the $BaTiO_3$ (60.9%) sample than in the TiO_2 (49.9%), which suggests more active sites (V_o) were formed in the $BaTiO_3$ catalyst, resulting in the higher CO_2 conversion using the $BaTiO_3$ catalyst.

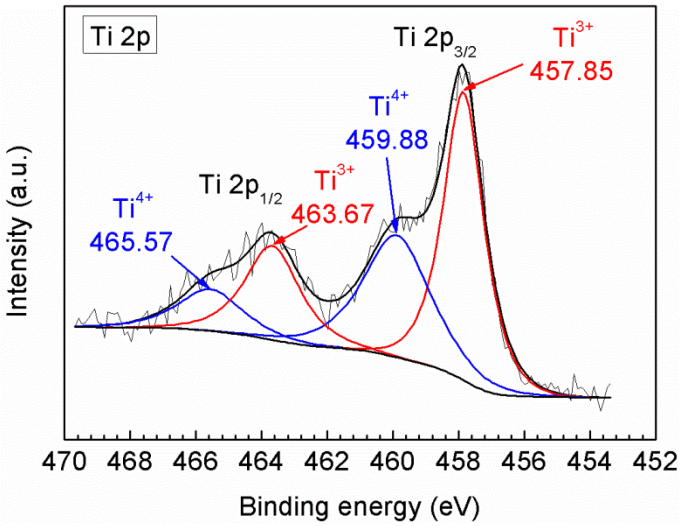

(a)

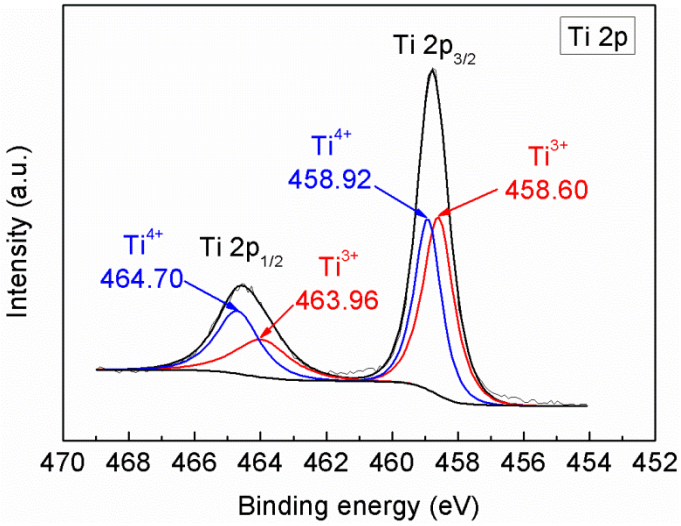

(b)

Fig. 6. XPS spectra of Ti 2p peaks for (a) $BaTiO_3$; (b) TiO_2

Moreover, the combination rate of electron-hole pairs can also be significantly reduced in a plasma-photocatalytic system due to the presence of the electric field and the interactions between the plasma and photocatalyst [59]. In this study, the process of plasma-photocatalytic conversion of CO_2 can be described by Fig. 7. The electron (e^-) - hole (h^+) pairs are generated with the aid of highly energetic electrons from the gas discharge, and are moved in the opposite direction by the electric field, which can

reduce the probability of recombination. In the electron transfer process, CO_2 adsorbed in the V_o is reduced to the anion radical $CO_2^{\bullet -}$ by electrons from e^--h^+ pairs (Eq.21), followed by the decomposition of $CO_2^{\bullet -}$ into CO and the occupation of one oxygen atom in the V_o site. The overall reaction is expressed in Eq.22 [55, 60], in which [Photocatalyst + V_o] and [Photocatalyst] represent the defective and defect-free photocatalysts, respectively.

$$CO_2 + e^- \rightarrow CO_2^{\bullet -} \quad (21)$$

$$CO_2 + [\text{Photocatalyst} + V_o] \rightarrow CO + [\text{Photocatalyst}] \quad (22)$$

$$4h^+ + 2O^{2-} \rightarrow O_2 \quad (23)$$

$$e^- + Ti^{4+} \rightarrow Ti^{3+} \quad (24)$$

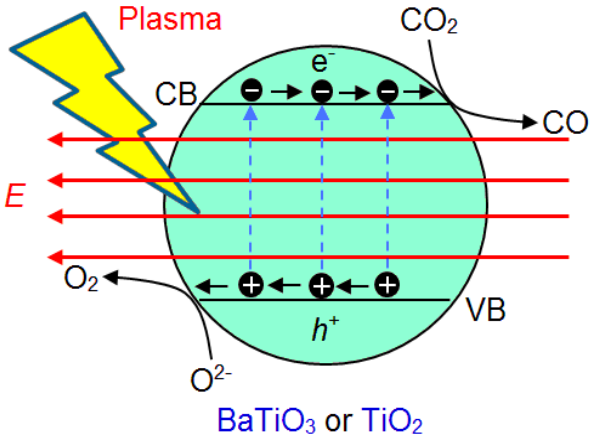

Fig. 7. Reaction mechanisms of plasma-photocatalytic conversion of CO_2 on the surface of photocatalysts

In addition, V_o can be regenerated by oxidizing the surface O^{2-} anions using holes, followed by releasing O_2, as shown in Eq. 23. To balance the charge, the Ti^{4+} in the vicinity of the regenerated V_o can be reduced to Ti^{3+} by electrons [55, 61, 62], as shown in Eq. 24. This cyclic healed-regeneration of the oxygen vacancies maintains the equilibrium of the active sites in the photocatalysts and controls the conversion of

406 CO_2, which can be confirmed by our experimental results as the CO_2 conversion did
407 not change significantly when the plasma discharge was on for nearly two hours.
408 Therefore, we find that the synergistic effect resulting from the integration of DBD
409 and photocatalysis for CO_2 conversion at low temperatures (without extra heating) can
410 be attributed to the physical effect induced by the presence of photocatalysts in the
411 discharge and the dominant photocatalytic surface reaction driven by the discharge.
412
413 **3.3. Energy efficiency**
414 Fig. 8 shows a comparison of the energy efficiency for CO_2 conversion using
415 different atmospheric pressure non-thermal plasmas. It is clear that the energy
416 efficiency (0.60 mmol/kJ) of the plasma CO_2 conversion in the presence of
417 photocatalysts ($BaTiO_3$) in this work is much higher than most of the other plasma
418 processes regardless of the catalyst used. As shown in Fig. 8, the maximum energy
419 efficiency of 0.69 mmol/kJ was achieved when the pure CO_2 decomposition was
420 performed in an AC gliding arc discharge at a feed flow rate of 1.31 L/min. However,
421 the corresponding conversion of CO_2 in this process was only 15.1%, which is
422 significantly lower than that (38.3%) obtained in this work. A balance between CO_2
423 conversion and energy efficiency in the plasma processing of CO_2 is significantly
424 important for the development and deployment of an efficient and cost-effective
425 plasma process for CO_2 conversion and utilization [17]. In this work, the combination
426 of DBD and photocatalysts ($BaTiO_3$ and TiO_2) leads to a significant enhancement in
427 the CO_2 conversion and energy efficiency of the plasma process, as well as a balance
428 between them. It is also interesting to note that the energy efficiency obtained in this
429 work (DBD) is much higher than that of similar chemical reactions using a
430 conventional packed bed DBD reactor where materials and/or catalysts are fully

packed into the discharge gap [63]. In our previous works, we found that packing catalysts into the entire discharge zone led to a strong packed-bed effect and was found to shift the discharge mode from a typical strong filamentary microdischarge across the gap to a combination of surface discharge and weak microdischarge due to a significant reduction in the discharge volume [6, 10, 64]. As a result, only limited surface discharge can be generated on part of the catalyst surface and spatially limited microdischarges generated in the void space between pellet-pellet and pellet-quartz wall [10, 40]. The formation of strong filamentary discharges in a DBD reactor without a catalyst is strongly suppressed when the solid catalysts are fully packed into the discharge gap. It is well known that a packed-bed effect can enhance the electric field in the plasma, which contributes to the enhancement of the reaction performance to some extent. However, such a significant transition in behaviour of the discharge mode induced by the strong packed bed effect (fully packed) could substantially reduce the performance of plasma-catalytic conversion or reforming processes for energy and fuel production, as catalysts placed in the plasma area cannot be fully interacted and activated by the spatially limited discharges and weak interactions between the plasma and catalyst [6, 10]. Our previous work has clearly shown that how to pack catalysts in a DBD reactor is of primary importance to induce strong physical and chemical interactions between the plasma and catalyst, which consequently affects the generation of the synergistic effect of the plasma-catalytic reaction, especially for the conversion of undiluted reactants to valuable fuels and chemicals [6].

One may argue that as packed-bed DBD reactors have been demonstrated to be effective at removing a wide range of low concentration (10-1000 ppm) environmental gas pollutants [43], they could also be beneficial in the conversion of undiluted

456 reactants. However, the major reaction mechanisms involved in the removal of dilute
457 and low concentration gas pollutants and in the conversion of undiluted reactants (e.g.
458 CO_2 or a mixture of CO_2 and CH_4) are significantly different due to different
459 concentrations of reactants in the plasma chemical reactions. In the former reactions,
460 highly energetic electrons mainly collide with carrier gas (e.g. air) to generate
461 chemically reactive species (e.g. O, O_3, OH and N_2(A)) which play dominant roles in
462 the stepwise decomposition and oxidation of low concentration (ppm level) pollutants
463 into CO, CO_2, H_2O and other by-products [65]. In contrast, electron impact reactions
464 with reactants (e.g. CO_2) make significant contributions to the conversion of undiluted
465 reactants in the latter reactions as carrier gases (e.g. N_2 and Ar) are not preferable. The
466 transition behaviour of the discharge mode resulting in weak interactions of plasma
467 and catalyst induced by the packed bed effect might not be so important in the former
468 reactions since the increased electric field in the packed bed DBD reactor might be
469 sufficient to produce reactive species for the removal of pollutants of ppm level. In
470 addition, even a catalyst support (e.g. γ-Al_2O_3 and SiO_2) placed in a packed bed DBD
471 reactor could absorb or decompose some gas pollutants of low concentration [66, 67],
472 leading us to think that the negative effect caused by the weak interaction between the
473 plasma and packing catalysts (or supports) might be insignificant in the removal of
474 dilute gas pollutants.

475 Further improvement in the energy efficiency of this process can be expected from
476 the optimization of the plasma power and the design of new catalysts (e.g. coating
477 metal nanoparticles on the photocatalysts). For example, previous simulation work has
478 suggested that the energy efficiency of a plasma reactor can be enhanced by a factor of
479 4 when using rectangular pulses instead of a sinusoidal voltage [68].

The high reaction rate and fast attainment of steady state in plasma processes allow rapid start-up and shutdown of the process compared to thermal treatment, whilst plasma systems can also work efficiently with a rather small and compact size. This offers flexibility for plasma-catalytic processes to be integrated with renewable energy sources such as waste energy from wind power, as the surplus energy could provide cheap waste electricity for powering the plasma-catalytic process, making it more effective in reducing CO_2 emissions.

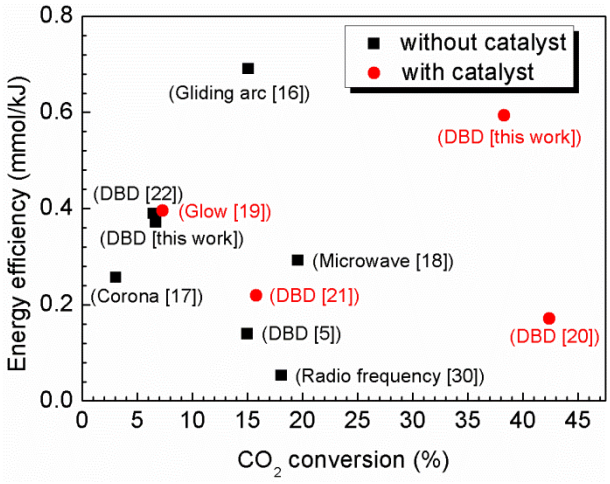

Fig. 8. Comparison of energy efficiency for CO_2 conversion with different atmospheric pressure plasma processes

4. Conclusions

In this study, plasma-photocatalytic conversion of CO_2 into CO and O_2 has been investigated using a DBD reactor combined with $BaTiO_3$ and TiO_2 photocatalysts. The combination of plasma with the $BaTiO_3$ and TiO_2 photocatalysts in the CO_2 DBD slightly increases the gas temperature of the plasma by 6-11 ^oC compared to the CO_2 discharge in the absence of a catalyst at a SED of 28 kJ/L, while the plasma gas temperature in the gas phase is almost the same as the temperature on the surface of

the photocatalysts ($BaTiO_3$ and TiO_2) in the plasma-catalytic DBD reactor. The combination of plasma with $BaTiO_3$ and TiO_2 catalysts has shown a synergistic effect, which significantly enhances the conversion of CO_2 and the energy efficiency by a factor of 2.5 compared to the plasma reaction in the absence of a catalyst. The presence of the catalyst pellets in the plasma gap is found to play a dominant role in inducing plasma physical effects, such as the enhancement of the electric field and production of more energetic electrons and reactive species, which in turn leads to chemical effects and partly contributes to the conversion of CO_2. We find that the intensity of UV emissions generated in the CO_2 DBD is significantly lower than that emitted from external UV sources (e.g. UV lamps) that are commonly used to activate photocatalysts in conventional photocatalytic reactions. This phenomenon suggests that the UV emissions generated by the CO_2 DBD only play a minor role in the activation of the $BaTiO_3$ and TiO_2 catalysts in the plasma-photocatalytic conversion of CO_2, and its contribution to the achieved exceptional performance of the plasma-photocatalytic reaction and the synergy of plasma-photocatalysis could be very weak or negligible. In this study, the highly energetic electrons generated by plasma have been considered as the main driving force to activate the photocatalysts for CO_2 conversion. The overall synergistic effect resulting from the integration of DBD with photocatalysis for CO_2 conversion at low temperatures (without extra heating) can be attributed to both the physical effect induced by the presence of the catalyst in the discharge and the dominant photocatalytic surface reaction driven by energetic electrons from the CO_2 discharge.

Acknowledgements

Support of this work by the UK EPSRC is gratefully acknowledged.

Appendix A. Supplementary material

Electronic Supplementary Information (ESI) available: [details of thermodynamic equilibrium calculation of CO_2 conversion and XRD patterns of photocatalysts are available].

References

[1] N.A.M. Razali, K.T. Lee, S. Bhatia, A.R. Mohamed, Renew. Sust. Energ. Rev. 16 (2012) 4951-4964.

[2] M. Tahir, N.S. Amin, Renew. Sust. Energ. Rev. 25 (2013) 560-579.

[3] N.S. Spinner, J.A. Vega, W.E. Mustain, Catal. Sci. Technol. 2 (2012) 19-28.

[4] R.W. Dorner, D.R. Hardy, F.W. Williams, H.D. Willauer, Energ. Environ. Sci. 3 (2010) 884-890.

[5] S. Paulussen, B. Verheyde, X. Tu, C. De Bie, T. Martens, D. Petrovic, A. Bogaerts, B. Sels, Plasma Sources Sci. Technol. 19 (2010) 034015.

[6] X. Tu, J.C. Whitehead, Appl. Catal. B-Environ. 125 (2012) 439-448.

[7] H.L. Chen, H.M. Lee, S.H. Chen, M.B. Chang, S.J. Yu, S.N. Li, Environ. Sci. Technol. 43 (2009) 2216-2227.

[8] H.L. Chen, H.M. Lee, S.H. Chen, Y. Chao, M.B. Chang, Appl. Catal. B-Environ. 85 (2008) 1-9.

[9] E.C. Neyts, B. A, J. Phys. D: Appl. Phys. 47 (2014) 224010.

[10] X. Tu, H.J. Gallon, M.V. Twigg, P.A. Gorry, J.C. Whitehead, J. Phys. D: Appl. Phys. 44 (2011) 274007.

[11] X. Tu, H.J. Gallon, J.C. Whitehead, Catal. Today. 211 (2013) 120-125.

[12] J. Van Durme, J. Dewulf, C. Leys, H. Van Langenhove, Appl. Catal. B-Environ. 78 (2008) 324-333.

[13] J.C. Whitehead, Pure Appl. Chem. 82 (2010) 1329-1336.

549 [14] S.L. Brook, M. Marquez, S.L. Suib, Y. Hayashi, H. Matsumoto, J. Catal. 180 (1998)
550 225-233.
551 [15] A. Indarto, J.-W. Choi, H. Lee, H.K. Song, Environ. Eng. Sci. 23 (2006) 1033-1043.
552 [16] A. Indarto, D.R. Yang, J.W. Choi, H. Lee, H.K. Song, J. Hazard. Mater. 146 (2007)
553 309-315.
554 [17] T. Mikoviny, M. Kocan, S. Matejcik, N.J. Mason, J.D. Skalny, J. Phys. D: Appl. Phys.
555 37 (2004) 64-73.
556 [18] M. Tsuji, T. Tanoue, K. Nakano, Y. Nishimura, Chem. Lett. (2001) 22-23.
557 [19] J.Y. Wang, G.G. Xia, A.M. Huang, S.L. Suib, Y. Hayashi, H. Matsumoto, J. Catal. 185
558 (1999) 152-159.
559 [20] S. Wang, Y. Zhang, X. Liu, X. Wang, Plasma Chem. Plasma Process. 32 (2012) 979-
560 989.
561 [21] Q.Q. Yu, M. Kong, T. Liu, J.H. Fei, X.M. Zheng, Plasma Chem. Plasma Process. 32
562 (2012) 153-163.
563 [22] G.Y. Zheng, J.M. Jiang, Y.P. Wu, R.X. Zhang, H.Q. Hou, Plasma Chem. Plasma
564 Process. 23 (2003) 59-68.
565 [23] D. Mei, Y.-L. He, S. Liu, J.D. Yan, X. Tu, Plasma Process. Polym. (2015) DOI:
566 10.1002/ppap.201500159.
567 [24] R. Aerts, W. Somers, A. Bogaerts, ChemSusChem. 8 (2015) 702-716.
568 [25] M. Ramakers, I. Michielsen, R. Aerts, V. Meynen, A. Bogaerts, Plasma Process. Polym.
569 12 (2015) 755-763.
570 [26] A. Baylet, P. Marecot, D. Duprez, X. Jeandel, K. Lombaert, J.M. Tatibouet, Appl. Catal.
571 B-Environ. 113 (2012) 31-36.
572 [27] H.B. Zhang, K. Li, T.H. Sun, J.P. Jia, Z.Y. Lou, L.L. Feng, Chem. Eng. J. 241 (2014)
573 92-102.

574 [28] R. Snoeckx, R. Aerts, X. Tu, A. Bogaerts, J. Phys. Chem. C. 117 (2013) 4957-4970.
575 [29] X. Tu, H.J. Gallon, J.C. Whitehead, J. Phys. D: Appl. Phys. 44 (2011) 482003.
576 [30] X. Tu, B. Verheyde, S. Corthals, S. Paulussen, B.F. Sels, Phys. Plasmas. 18 (2011)
577 080702.
578 [31] L.F. Spencer, A.D. Gallimore, Plasma Chem. Plasma Process. 31 (2011) 79-89.
579 [32] A. Fridman, Plasma Chemistry, Cambridge University Press, New York, 2008.
580 [33] R. Aerts, T. Martens, A. Bogaerts, J. Phys. Chem. C. 116 (2012) 23257-23273.
581 [34] X.B. Zhu, X. Gao, C.H. Zheng, Z.H. Wang, M.J. Ni, X. Tu, RSC Adv. 4 (2014) 37796-
582 37805.
583 [35] F. Brehmer, S. Welzel, M.C.M. van de Sanden, R. Engeln, J. Appl. Phys. 116 (2014)
584 123303.
585 [36] I.A. Semiokhin, Y.P. Andreev, Russ. J. Phys. Chem., 40 (1966) 1161.
586 [37] H.H. Kim, A. Ogata, S. Futamura, IEEE Trans. Plasma Sci. 34 (2006) 984-995.
587 [38] T. Hammer, T. Kappes, M. Baldauf, Catal. Today. 89 (2004) 5-14.
588 [39] H.J. Gallon, H.H. Kim, X. Tu, J.C. Whitehead, IEEE Trans. Plasma Sci. 39 (2011)
589 2176-2177.
590 [40] X. Tu, H.J. Gallon, J.C. Whitehead, IEEE Trans. Plasma Sci. 39 (2011) 2172-2173.
591 [41] W.S. Kang, J.M. Park, Y. Kim, S.H. Hong, IEEE Trans. Plasma Sci. 31 (2003) 504-510.
592 [42] M. Zaka-ul-Islam, K. Van Laer, A. Bogaerts, 31th International Conference on
593 Phenomena in Ionized Gases Granada, Spain, 2013.
594 [43] H.L. Chen, H.M. Lee, S.H. Chen, M.B. Chang, Ind. Eng. Chem. Res. 47 (2008) 2122-
595 2130.
596 [44] O. Guaitella, L. Gatilova, A. Rousseau, Appl. Phys. Lett. 86 (2005) 151502.
597 [45] L.G. Devi, G. Krishnamurthy, J. Phys. Chem. A. 115 (2011) 460-469.

[46] C. Subrahmanyam, M. Magureanu, D. Laub, A. Renken, L. Kiwi-Minsker, J. Phys. Chem. C. 111 (2007) 4315-4318.

[47] O. Guaitella, F. Thevenet, E. Puzenat, C. Guillard, A. Rousseau, Appl. Catal. B-Environ. 80 (2008) 296-305.

[48] A. Cybula, M. Klein, A. Zaleska, Appl. Catal. B-Environ. 164 (2015) 433-442.

[49] S. Xie, Y. Wang, Q. Zhang, W. Deng, Y. Wang, ACS Catal. 4 (2014) 3644-3653.

[50] A.A. Assadi, A. Bouzaza, S. Merabet, D. Wolbert, Chem. Eng. J. 258 (2014) 119-127.

[51] A.A. Assadi, J. Palau, A. Bouzaza, J. Penya-Roja, V. Martinez-Soriac, D. Wolbert, J. Photoch. Photobio. A. 282 (2014) 1-8.

[52] T. Sano, N. Negishi, E. Sakai, S. Matsuzawa, J. Mol. Catal. A-Chem. 245 (2006) 235-241.

[53] A.E. Wallis, J.C. Whitehead, K. Zhang, Catal. Lett. 113 (2007) 29-33.

[54] I. Nakamura, N. Negishi, S. Kutsuna, T. Ihara, S. Sugihara, E. Takeuchi, J. Mol. Catal. A-Chem. 161 (2000) 205-212.

[55] L.J. Liu, Y. Li, Aerosol Air Qual. Res. 14 (2014) 453-469.

[56] X.Y. Pan, M.Q. Yang, X.Z. Fu, N. Zhang, Y.J. Xu, Nanoscale, 5 (2013) 3601-3614.

[57] N.A. Deskins, R. Rousseau, M. Dupuis, J. Phys. Chem. C. 115 (2011) 7562-7572.

[58] L.J. Liu, C.Y. Zhao, Y. Li, J. Phys. Chem. C. 116 (2012) 7904-7912.

[59] A. Mizuno, Y. Kisanuki, M. Noguchi, S. Katsura, S.H. Lee, U.K. Hong, S.Y. Shin, J.H. Kang, IEEE Trans. Ind. Appl. 35 (1999) 1284-1288.

[60] W. Pipornpong, R. Wanbayor, V. Ruangpornvisuti, Appl. Surf. Sci. 257 (2011) 10322-10328.

[61] L.B. Xiong, J.L. Li, B. Yang, Y. Yu, J. Nanomater. (2012) 831524.

[62] A. Fujishima, T.N. Rao, D.A. Tryk, J. Photochem. Photobiol. C: Photochem. Rev. 1 (2000) 1-21.

[63] D.H. Mei, X.B. Zhu, Y.L. He, J.D. Yan, X. Tu, Plasma Sources Sci. Technol. 24 (2015) 015011.

[64] H.J. Gallon, X. Tu, J.C. Whitehead, Plasma Process. Polym. 9 (2012) 90-97.

[65] X.B. Zhu, X. Gao, R. Qin, Y.X. Zeng, R.Y. Qu, C.H. Zheng, X. Tu, Appl. Catal. B-Environ. 170 (2015) 293-300.

[66] A.E. Wallis, J.C. Whitehead, K. Zhang, Appl. Catal. B-Environ. 74 (2007) 111-116.

[67] A.E. Wallis, J.C. Whitehead, K. Zhang, Appl. Catal. B-Environ. 72 (2007) 282-288.

[68] T. Martens, A. Bogaerts, J. van Dijk, Appl. Phys. Lett. 96 (2010) 131503.